ARTICLE NO. 79-4062

Stability Analysis of a Flexible Spacecraft with a Sampled-Data Attitude Sensor

Subhash Garg*
University of Toronto, Toronto, Ontario, Canada

The pitch attitude control system for a flexible communications satellite is analyzed using sampled-data techniques. The sampling arises mainly from the use of discrete-time attitude measurement rather than from the digital controller implementation. It is found that Nyquist techniques lead to a relatively simple stability analysis that models the multirate sampling process with considerable fidelity, eliminating guesswork associated with equivalent delays. Controller modifications that improve stability are arrived at by this route. Finally, flexible-mode frequency and damping are varied to evaluate their influence on stability. There seems to exist a critical frequency at which stability margins are very small. Increasing the damping, predictably, improves matters.

I. Introduction

INCREASING performance requirements, a relatively benign environment, and prohibitive weight costs combine to make attitude control of flexible spacecraft a challenging and frequently faced problem. Two factors seem common to many control analyses of this problem. The first is the use of normal modes to represent spacecraft dynamics, an approach that is tenable under quite reasonable circumstances.[1] The second is the use of continuous time techniques for the analysis and design of control systems. Although the reliability and versatility of digital electronics may dictate discrete-time control, the analysis can be continuous, the simulation discrete, and the hardware designed to approximate a continuous controller. Such was the case, for example, with the communications technology satellite (CTS), in which the author was involved in a small way.

Discrete-time design methods have been applied in some recent work. Digital redesign of a continuous controller was applied to the spinning Skylab by Kuo[2] and experience with discrete methods applied to attitude control with lightly damped vibration modes is reported by Folgate.[3] In both cases, significant advantages were noted. A review of analysis methods for digital flight control is provided by Slater.[4] Control theory for discrete-time systems is well developed from both modern[5] and classical[6] viewpoints. Its application is usually straightforward, and may be required even when the electronics clock rate is high enough to warrant a continuous approximation. The purpose of this paper is to show such an example which applies to a real satellite.

II. Pitch Control of Hermes

The Hermes (CTS) spacecraft is equipped with flexible solar arrays, and flexibility was an important design consideration for it from the beginning. Pitch control is exercised by a momentum wheel and a linear, integral plus lead-lag controller, as described by Millar,[7] who applied continuous time techniques for stability analysis in the presence of flexibility. A schematic of the single-axis pitch control system is shown in Fig. 1. The control electronics use high-speed (clock rate 3310 Hz) digital differential analyzers, well approximated by continuous transfer functions. The flexible spacecraft dynamics typically includes one mode. We have then the transfer functions:

$$G_c(s) = \left(\frac{nK_I}{s} + \frac{\tau_0 s + 1}{\tau_0 s/n + 1}\right)\left(\frac{1}{n}K_p e^{-\frac{1}{2}T_p s}\right)$$

$$G_m(s) = \frac{K_T s}{s + \omega_m}$$

$$G_d(s) = \frac{1}{I_y}\left(\frac{1}{s^2} + \frac{K_A}{s^2 + 2\zeta\omega_A s + \omega_A^2}\right) \tag{1}$$

The K_p term in G_c approximates a pulse width modulator. The functions $h(s)$ and $A(s)$ depend on the modeling of the scanning infrared horizon sensor. Its operation may be explained by means of the diagram of Fig. 2. One scan takes T seconds and produces one raw sample of attitude. Four samples are averaged, yielding an output every $4T$ seconds. The control electronics then samples the output register every $5T$ seconds. Since the two outputs agree every $20T$, this is the effective sampling period as discussed later. Since T is about 0.25 s, this process is easily seen to be significant. It was heuristically replaced by Millar[7] with a pure time delay, an approach that is improved upon here. The equivalent delay concept is representative of design methods used for this controller.

Continuous Case

If we ignore the sampling, the sensor averaging transfer function $A(s)$ is:

$$A(s) = \left(1 + e^{-Ts} + e^{-2Ts} + e^{-3Ts}\right)/4 \tag{2}$$

A continuous stability analysis can be easily and directly made by means of Nyquist plots. For systems with poles at the origin, the interpretation of these plots is simplified if, instead of the modulus γ and argument θ, one plots $\tan^{-1}(\gamma)$ vs θ.

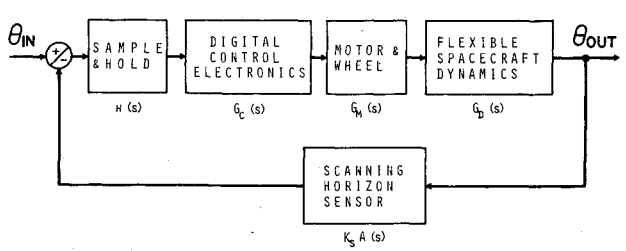

Fig. 1 Schematic of CTS pitch controller.

Received Feb. 28, 1978; revision received July 18, 1978.

*Index category: Spacecraft Dynamics and Control.

*Research Associate, Institute for Aerospace Studies. Member AIAA.

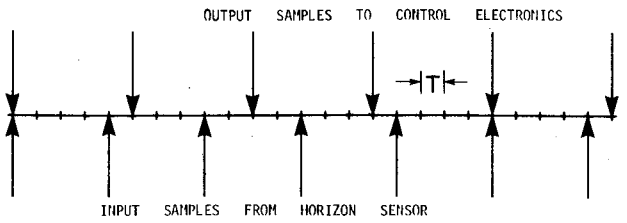

Fig. 2 Horizon sensor time line.

This reduces the point at infinity to a finite circle, leaving the number of encirclements unchanged. Thus modified, the Nyquist plot of the continuous system, for the configuration defined by the numerical values in Table 1, is shown in Fig. 3a. The system is seen to be stable, and numerical calculations show that it has a gain margin of 36 dB and a phase margin of 30 deg. Since a pure delay rotates the Nyquist plot clockwise, the system will obviously become unstable at some point. With a delay of $5T/2$ (Fig. 3b), corresponding to a zero-order hold, stability is preserved, but the phase margin is a mere 5 deg; with a somewhat larger delay the system becomes unstable. The point is that the correct value of the equivalent delay is difficult to determine in advance. Indeed, underestimation of the "equivalent loop delay" did occur during the design of Hermes and was corrected at a late stage.

III. Horizon Sensor Model

Let us now investigate the stability with a realistic sensor model. To this end, we observe from Fig. 2, the following:

1) The input and output samples coincide every $20T$ s. In this period, there are four output samples.

2) The second output sample is obtained by advancing the input sample by $4T$, sampling it (at the $20T$ rate), delaying the sample by $5T$ s and then holding it for $5T$ s. Similarly, other intermediate samples in the $20T$ period can be obtained.

Thus by the well-known advance-delay method,[6] the nonsynchronous sampling can be modeled. Including this in the system, the block diagram of Fig. 4 is obtained. Most transfer functions shown are as before, and

$$h(s) = \left(1 - e^{-5Ts}\right)/s$$

$$a_i(s) = e^{\alpha_i s} \qquad d_i(s) = e^{-\delta_i s} \tag{3a}$$

$$\alpha_i = (0,\ 4T,\ 8T,\ 12T)$$

$$\delta_i = (0,\ 5T,\ 10T,\ 15T) \tag{3b}$$

completes the model. It is noted that we have now raised the effective sampling period to $20T$ (about half the flexible mode period), so that significant interaction between flexibility and sampling may be expected.

IV. Sampled-Data Stability Analysis

The stability of sampled-data control systems can be analyzed using z transforms and root loci in the complex plane. This approach is cumbersome for the system of Fig. 4. On the other hand, the Nyquist criterion, when applied to study the stability of the standard feedback control system, gives the characteristic equation

$$1 + \overline{HG}^*(s) = 0 \tag{4}$$

where

$$\overline{HG}^*(s) = \frac{1}{T}\sum_{k=-\infty}^{\infty} \overline{HG}(s + jk\omega_s) \tag{5}$$

and $\omega_s = 2\pi/T$ is the sampling frequency. Equation (5) is valid if the sum converges and there is no jump discontinuity at $t = 0$ in the response. Equation (4) applies for stability of the sampled output. The sampled Laplace transform defined in Eq. (15) (designated by an asterisk) can be applied to any sampled function. The overbar denotes that all symbols under it have continuous, not sampled, interconnections and hence are evaluated at the same value of s.

For the system of Fig. 4, which has multiple sampled paths, the following approach is taken. We have

$$E_j(s) = a_j(s)A(s)\left[R(s) - K_s C(s)\right] \tag{6a}$$

where the output transform $C(s)$ is given by

$$C(s) = \sum_{i=1}^{m} \overline{hG_c G_m G_d d_i}(s) E_i^*(s) \tag{6b}$$

Hence

$$E_j(s) = \overline{a_j AR}(s) - \sum_{i=1}^{m} K_s \overline{a_j AhG_c G_m G_d d_i}(s) E_i^*(s) \tag{7}$$

Taking the sampled transform of this equation as defined in Eq. (5), the following matrix equation results:

$$\left[\delta_{ij} + K_s \overline{a_j AhG_c G_m G_d d_i^*}(s)\right] E_j^*(s) = \overline{a_j AR^*}(s) \tag{8}$$

where δ_{ij} is the Kronecker delta. This is a matrix equation for $E_j^*(s)$. The stability of the system is determined by the determinant of the matrix in Eq. (8), denoted by $\Delta^*(s)$. Its evaluation requires summing a convergent complex series to specified precision. The characteristic equation may be written

$$1 + (\Delta^*(s) - 1) = 0 \tag{9}$$

This is in the familiar form where Nyquist's theorem can be applied. The theorem remains applicable even for Δ^* not a rational polynomial fraction. It should be noted that the preceding approach does not guarantee the absence of hidden oscillations in the output. However, such oscillations will die out with time if the system is shown to be asymptotically stable.

It is clear from Eq. (9) that we can plot $(\Delta^*(s) - 1)$ and interpret the results similarly to a Nyquist plot. A sum like Eq. (5) has the following properties:

$$G^*(s + jm\omega_s) = G^*(s) \qquad (m \text{ integer}) \tag{10a}$$

$$G^*(\sigma \pm \tfrac{1}{2}j\omega_s) = \text{real} \tag{10b}$$

Due to the periodicity of G^*, we need evaluate Δ^* only from $s = -\frac{1}{2}j\omega_s$ to $s = \frac{1}{2}j\omega_s$. The Nyquist path is completed by going along the line $\sigma + \frac{1}{2}j\omega_s$ to infinity and back along $\sigma - \frac{1}{2}j\omega_s$. On these lines $\Delta^*(s)$ is real and decreases smoothly to unity.

Table 1 Nominal numerical values

n	Lead-lag ratio	20.0
I_y	Spacecraft pitch inertia, kg-m^2	90.2
K_A	Flexible mode gain	0.054
K_I	Integral gain coefficient	4.926E-4
K_p	PWM gain coefficient	29.00
K_s	Horizon sensor gain	$180/\pi$
K_T	Motor torque gain, N-m	0.00847
T	Horizon scan period, s	0.2475
ζ	Modal damping ratio	0.001
τ_0	Lead time constant, s	39.6
ω_A	Flexible mode frequency, Hz	0.1
$1/\omega_m$	Motor time constant, s	1440

V. Results – Controller Effects

Before presenting the results of the preceding analysis, it is useful to consider the case when the sampling of the horizon

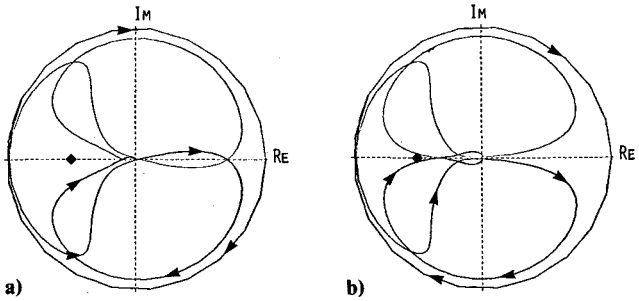

Fig. 3 Nyquist plots for continuous case: a) without delay, b) delay = $5T/2$.

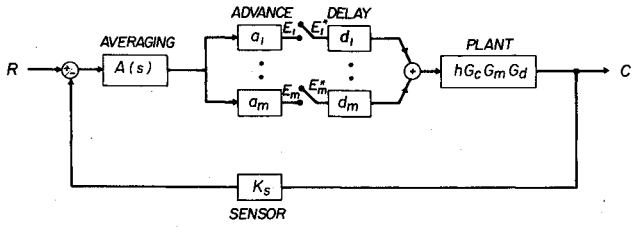

Fig. 4 Block diagram of detailed sampling model.

sensor output is synchronized with its attitude computation, i.e., no advance-delay method is required.

Synchronous Sampling

In this case, Fig. 4 applies with $m=1$ and $a_1(s)=d_1(s)=1$. Now we have just the characteristic equation (4). The sampling period is taken to be $5T$ s. The Nyqist plot for this case is shown in Fig. 5a. It is clearly seen that even with this approximate model of sampling, the system shown to be stable in the continuous case (Fig. 3a) is distinctly unstable. The effective phase shift produced by sampling considerably exceeds that corresponding to a zero-order hold (Fig. 3b).

This instability became apparent in the CTS project partly as a result of the analysis presented here. Perhaps the most effective solution to the problem is to increase the lead-lag ratio n, as can be inferred even from a continuous analysis. For comparison, Fig. 5b shows the results of increasing n to 40 from 20. The stabilization is also partly due to a gain reduction, evident from Eq. (1).

Multirate Sampling

With the detailed sensor model approach of Eq. (9), we have $m=4$ and numerical values from Eq. (3b) for the advance-delay parameters. The determinant $\Delta^*(s)$ is obtained by direct expansion, and the series in Eq. (8) are summed until the relative error incurred by neglecting the next term is less than $1.E\text{-}5$, in terms of modulus. The results are shown in Fig. 6a.

Instability is again apparent. In Fig. 6b we show the effect of another controller modification; namely, doubling the controller update frequency. Thus one output sample is taken from the pitch sensor register every $5T/2$, rather than $5T$ s. In this case, we require eight advance-delay loops, and the 8×8 determinant is evaluated by triangularization using complex Gauss elimination. The α_i and δ_i are now

$$\alpha_i = (0,\ 0,\ 4,\ 4,\ 8,\ 12,\ 12,\ 16)T$$

$$\delta_i = (0,\ 2.5,\ 5,\ 7.5,\ 10,\ 12.5,\ 15,\ 17.5)T \qquad (11)$$

It is seen from Fig. 6b that this considerable modification does not yield stability. This shows the value of the sampled-data analysis, since intuitively one might expect the "equivalent delay" to be greatly reduced. It should also be noted that the detailed model results with $n=40$ (Fig. 7a), although showing stability, yield a smaller margin of stability than the synchronous sampling approximation (Fig. 5b). The doubled controller update frequency case (Eq. 11) will not be discussed further.

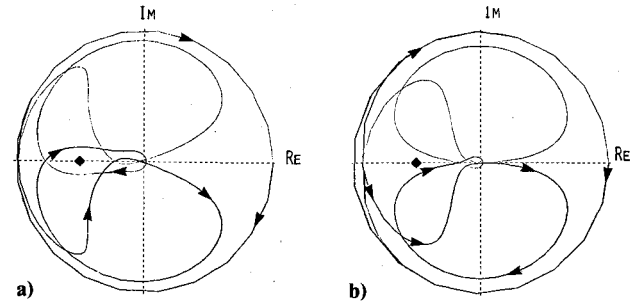

Fig. 5 Stability with synchronized sampling, period = $5T$: a) nominal case, b) ratio n increased to 40.

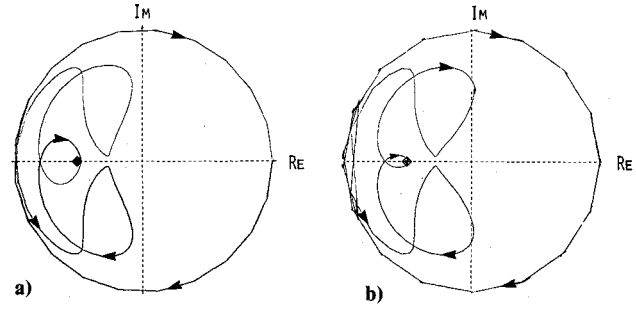

Fig. 6 Stability with detailed sampling model: a) nominal, b) doubled controller input frequency.

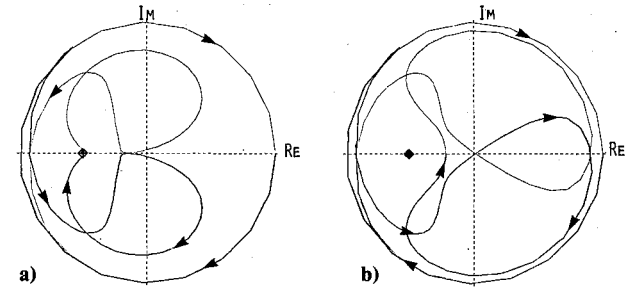

Fig. 7 Effect of flexible mode frequency ratio $R=2\omega_A/\omega_s$: a) $R=0.99104$, nominal, b) $R=0.5$.

VI. Results – Flexibility Effects

In this section the stability results given by the detailed sensor model are explored in the flexibility parameter space. The first parameter of interest is the mode frequency ω_A. We consider $n=40$ throughout this section. The results for nominal ω_A are shown in Fig. 7a. One parameter of interest is the ratio of ω_A and the Nyquist frequency, $R\equiv 2\omega_A/\omega_s$. The nominal case (Fig. 7a) has $R=0.99104$, and the results for $R=0.500$ are shown in Fig. 7b for comparison. We have the somewhat unconventional result that lowering the flexible-mode frequency improves stability. In a continuous analysis, this phenomenon is usually explained by postulating an equivalent time delay, which produces larger phase lags at higher frequencies.

The interaction between sampling and flexibility may be explored further in the region $R\approx 1$. Increasing ω_A from the nominal value, the cases $R=0.993$ and $R=0.998$ are shown in Fig. 8. We see that the Nyquist plot and the margin of stability are very sensitive to the flexible-mode frequency. Figure 8a shows the most critical case, at $R=0.993$, when the -1 point is approached within 1%. Evidently, $\Delta^*(s=\frac{1}{2}j\omega_s)$ is close to

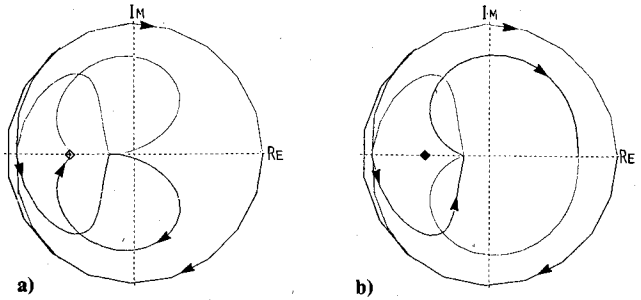

Fig. 8 Stability changes near $R = 1$: a) $R = 0.993$, b) $R = 0.998$.

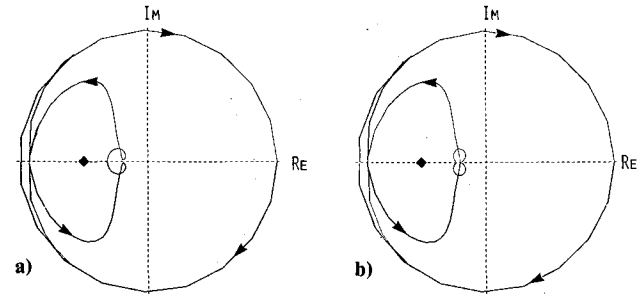

Fig. 9 Effect of other modal parameters: a) damping increased to 0.010, b) gain reduced to 0.002.

zero for this R, while for $R = 0.998$ (Fig. 8b), it is quite large. For $R = 1$, as expected, it was found that $\Delta^*(s)$ has a pole near $\frac{1}{2}j\omega_s$. The zeroes of a sampled transfer function, unlike the poles, bear no simple relation to those of its continuous version. However, it is clear that $\Delta^*(s)$ has a zero near $\frac{1}{2}j\omega_s$ which changes to a pole as R goes from 0.993 to 1.0. The closeness of these two values is not unexpected in view of the extremely small damping ($\zeta = 0.001$) and small gain ($K_A = 0.054$).

Although the destabilizing influence of flexibility is clear from the preceding, the extent of its effect depends crucially on the damping ratio. The nominal case (with $n = 40$) with ζ increased to 0.01 is shown in Fig. 9a. Similarly, Fig. 9b shows the case $K_A = 0.002$, representative of a spacecraft with extremely small appendages. In both cases, it is seen that stability margins are much improved. In practical terms this means that adequate structural damping alleviates the control problem substantially, so much so that an artificial damper may be an attractive design solution.

VII. Concluding Remarks

In the present investigation it has been shown that the sampling nature of current attitude sensors and digital electronic implementation of controllers can only be ignored at the designer's peril. The heuristic approach of inserting an equivalent delay in a conventional continuous-time analysis can become unsafe or too conservative. It is not particularly difficult to use sampled-data techniques at least for analysis and validation of a system designed in continuous fashion, and the Nyquist criterion is especially convenient here. We have seen that the effect of delay on lightly damped flexible modes is significant in that lowering the frequency can actually improve stability. The case when ω_A is close to the Nyquist frequency has been studied in detail.

It should also be remarked that the use of discrete-time techniques for a priori control system design is quite feasible and may be attractive for it simplifies implementation as well. It may well be possible to get away with much lower controller sampling rates than required to maintain a continuous-time approximation.

Acknowledgments

The author's work on this paper was supported by a Special Project Grant from the National Research Council of Canada. The problem studied arose from an earlier association with Spar Aerospace Products Ltd.

References

[1] Hughes, P.C., "Dynamics of Flexible Space Vehicles with Active Attitude Control," *Celestial Mechanics,* Vol. 9, 1974, pp. 21-39.

[2] Kuo, B.C., Seltzer, S.M., Singh, G., and Yackel, R.A., "Design of a Digital Controller for Spinning Flexible Spacecraft," *Journal of Spacecraft and Rockets,* Vol. 11, Aug. 1974, pp. 584-589.

[3] Folgate, K., "Discrete-Time Attitude Control of Spacecraft Containing Low-Frequency Lightly Damped Flexible Modes," AIAA Paper 76-262, April 1976.

[4] Slater, G.L., "A Unified Approach to Digital Flight Control Algorithms," AIAA Paper 74-884, Aug. 1974.

[5] Kwakernak, H. and Sivan, R., *Linear Optimal Control Systems,* Wiley-Interscience, New York, 1972, Chap. 6.

[6] Tou, J., *Digital and Sampled-Data Control Systems,* McGraw-Hill, New York, 1959, pp. 281-308.

[7] Millar, R.A. and Vigneron, F.R., "The Effect of Structural Flexibility on the Stability of Pitch for the Communications Technology Satellite," Canadian Conference on Automatic Control, Vancouver, Canada, June 1975.